Application of the LCPT Model to Solid-Liquid Equilibria for Binary Compound-Forming Alloys

Wayne J. Howell
Packaging Development Laboratory, International Business Machines Corp., Hopewell Junction, NY 12533
Montgomery M. Alger
Corporate Research and Development Center, General Electric Co., Schenectady, NY 12301
Charles A. Eckert
School of Chemical Engineering, Georgia Institute of Technology, Atlanta, GA 30332

The linear chemical-physical theory (LCPT) model for liquid metal solution thermodynamics has been extended to the determination of the liquidus curves for binary intermetallic compound-forming systems. The equations developed include corrections to the observed melting point temperature and heat of fusion for compounds that dissociate partially on melting. The primary advantages of the LCPT model for solid-liquid equilibria are the small number of physically realistic parameters required, ease of implementation, and wide applicability. In addition, the model also permits the incorporation of compounds in modeling the liquidus curves that are not necessary for representing the liquid-phase thermodynamic properties. For the seven systems studied, the agreement between calculated and experimentally measured liquidus curves is quite good.

Introduction

The accurate representation of solid-liquid equilibrium (SLE)-phase diagrams for binary and multicomponent metal systems requires a liquid solution model that can represent accurately the activities and partial molar enthalpies of species in solution. Liquid alloys exhibit a wide range of thermodynamic behavior, from strong positive deviations from Raoult's law, resulting in liquid immiscibility, to large negative deviations caused by intermetallic compound formation. To represent adequately the thermodynamic properties of these solutions, a model must incorporate explicitly the important characteristics of these solutions. Chemical theory has been used successfully to model the thermodynamic properties of liquid metal solutions that exhibit evidence of intermetallic compound formation (Jordan, 1970, 1976, 1979; Bhatia and Hargrove, 1974; Bhatia et al., 1974; Predel and Oehme, 1974; Sommer, 1978, 1982a,b, 1983; Predel, 1979; Alger and Eckert, 1983, 1986a,b; Eckert et al., 1983; Gerling et al., 1983; Stoicos and Eckert, 1985; Howell et al., 1988; Howell and Eckert, 1988). The linear chemical-physical theory (LCPT) model (Howell et al., 1988) represented a major advance in minimizing the number of model parameters needed to represent the solution thermodynamics of a wide range of liquid metal systems.

In this article, the LCPT model is extended to the calculation of the liquidus curves for several binary compound-forming metal mixtures. The necessary equations for describing the phase boundary are developed. Corrections to the observed melting point and heat of fusion can be quite large and need to be considered when data are regressed and correlated; these are calculated based on the degree of dissociation that occurs on melting. A unique feature of using the LCPT model is that compounds other than those used to represent the liquid solution thermodynamics can be accounted for in representing the liquidus curve.

Chemical Theory Approach

The basic feature of a chemical theory model is the assumption that the intermetallic compounds are in dynamic equilibrium with the atomic elements (or monomers) making up the compound according to an expression of the form:

Correspondence concerning this article should be addressed to C. A. Eckert.

$$a_iA + b_iB = A_{a_i}B_{b_i} \tag{1}$$

for which an equilibrium constant for compound *i*, K_i, can be defined. The solution (called the true solution) is then treated as a multicomponent mixture of the monomers and compounds. The activities of the monomers are related to the experimentally observed activities through an expression derived by Prigogine and Defay (1954):

$$x_i\gamma_i = z_i\alpha_i \tag{2}$$

where x_i is the atom fraction of monomer *i* in the experimentally observed (or apparent) solution and γ_i is the experimentally observed activity coefficient. In the true solution, z_i is the true mole fraction, and α_i is the true activity coefficient of species *i*.

The equilibrium constant for compound *i*, K_i, is the product of a true composition equilibrium constant, K_{z_i}, and a true activity coefficient equilibrium constant, K_{α_i}:

$$K_i = \frac{z_{A_{a_i}B_{b_i}}}{z_A^{a_i} z_B^{b_i}} \cdot \frac{\alpha_{A_{a_i}B_{b_i}}}{\alpha_A^{a_i}\alpha_B^{b_i}} = K_{z_i}K_{\alpha_i} \tag{3}$$

This allows the separation of the excess Gibbs energy into two contributions, chemical and physical:

$$g^E = g^E_{\text{chem}} + g^E_{\text{phys}} \tag{4}$$

The chemical interactions are contained in K_{z_i} and the physical interactions are in K_{α_i}. In the LCPT model, the physical interactions are a function of the apparent atom fractions and are modeled using a single-parameter Scatchard-type expression (1931):

$$g^E_{\text{phys}} = A\Phi_A\Phi_B(x_Av_A + x_Bv_B) \tag{5}$$

where *A* is the physical-interaction model parameter, Φ_i is the volume fraction of component *i* based on the apparent solution composition, and v_i is the molar volume of component *i*. The chemical interactions are modeled using a group contribution approach, in which the Gibbs energies of formation for the postulated compounds are related linearly to the number of atoms comprising the compounds:

$$g^f_{i,\text{chem}} = -RT\ln K_{z_i} = (n_i - 1)G_g \tag{6}$$

where G_g is the single chemical-interaction model parameter, n_i is the number of atoms comprising compound *i*, and $g^f_{i,\text{chem}}$ is the Gibbs energy of formation for compound *i*. Only a single chemical-interaction parameter is required, regardless of the number of compounds postulated to exist in the true solution. Thus, there are only two model parameters for each binary, G_g and *A*, and, as with other chemical theory models, these two parameters are determined by fitting experimental activity coefficient data.

The temperature dependence of the Gibbs energy is also modeled using the LCPT model by taking the temperature derivatives of Eqs. 5 and 6. Two additional model parameters are introduced, one chemical and one physical, which are determined by fitting either experimental partial molar enthalpy data or integral enthalpy of mixing data. For this study, the temperature dependence of the enthalpies was not considered. This restriction could easily be relaxed at the cost of introducing two additional model parameters, but the accuracy of liquid metal thermodynamic data rarely justify more parameters.

Liquid-Phase Thermodynamic Properties

The LCPT model was used to represent the liquid metal activities (Gibbs energy) and enthalpies of the systems considered in this article. Table 1 lists the systems considered, the compounds postulated to exist in the liquid phase, and the Gibbs energy and enthalpy model parameters. Table 2 provides the sources for the experimental Gibbs energy and enthalpy data.

Solid-Liquid Equilibrium

For simplicity, we assume that the solid phases in equilibrium with the liquid phase are pure: that is, there is negligible dissolution of atomic elements *A* and *B* in the solid phases. This assumption can be relaxed for systems in which solid solutions form by including the Gibbs energy of mixing in the solid phase and extending the equations given below.

Determination of the liquidus curves begins by equating the fugacity of component *i* in the solid phase to that in the liquid phase:

Table 1. LCPT Model Parameters for Liquid-Phase Properties

		Gibbs Energy			Enthalpy		
System	Compound	*T* K	G_g kJ/mol	*A* 10^3 kJ/m^3	*T* K	H_g kJ/mol	*B* 10^3 kJ/m^3
In-Sb	In_3Sb	900	−0.730	−757.5	900	−5.19	−628.8
Cd-Sb	CdSb Cd_3Sb_2	773	−6.31	77.1	773	−6.16	997.3
Mg-Pb	MgPb Mg_2Pb	923	−15.04	−318.8	943	−19.14	18.96
Mg-Sn	MgSn Mg_2Sn	1,073	−14.67	−1,611.0	1,073	−30.46	−224.0
Mg-Ge	Mg_2Ge Mg_3Ge_2	1,388	−16.10	−2,766.0	1,388	−47.61	−510.9
Au-Sn	AuSn Au_2Sn	823	−7.73	−2,639.0	823	−14.36	−4,544.0
Ga-Mg	GaMg $GaMg_2$	923	−10.13	−1,356.0	923	−17.26	−2,124.0

Table 2. Sources for Liquid-Phase Properties

System	Gibbs Energy	Enthalpy
In-Sb	Hultgren et al. (1973)	Hultgren et al. (1973)
Cd-Sb	Geffken et al. (1967)	Geffken et al. (1967)
Mg-Pb	Eckert et al. (1983)	Sommer et al. (1980)
Mg-Sn	Eckert et al. (1983)	Sommer et al. (1980)
Mg-Ge	Eldridge et al. (1966)	Eldridge et al. (1966)
Au-Sn	Hultgren et al. (1973)	Hultgren et al. (1973)
Ga-Mg	Hultgren et al. (1973)	Hultgren et al. (1973)

$$f_{i(\text{pure solid})} = z_i \alpha_i f_i^o \tag{7}$$

where z_i is the true mole fraction of component i in the liquid phase, α_i is the liquid-phase true activity coefficient, f_i^o is the standard-state fugacity to which α_i refers, and $f_{i(\text{pure solid})}$ is the fugacity of component i as a pure solid. Prausnitz et al. (1986) discussed the relationship between the solid and liquid state fugacities from which the following relationship can be derived for determining the temperature-composition curve for each component:

$$\frac{1}{T} = \frac{1}{T_i^{mp}} - \frac{R}{\Delta h_i^{s-l}} \ln z_i \alpha_i \tag{8}$$

where T is the melting point temperature for component i in solution at a composition z_i, T_i^{mp} is the melting point of pure component i, and Δh_i^{s-l} is the heat of fusion of pure component i. Equation 8 is derived assuming that pure i in the solid phase goes to pure i in the liquid phase with no dissociation. Dissociation on melting produces an equilibrium distribution of monomers and compounds in the liquid phase, which results in a melting point depression due to the presence of monomers A and B. For example, a system with a congruently melting compound AB at the observed melting point will have the phase transition:

$$AB_{(s)} = AB_{(l)} + A_{(l)} + B_{(l)} \tag{9}$$

However, the heat of fusion required for Eq. 8 is for the phase transition:

$$AB_{(s)} = AB_{(l)} \tag{10}$$

When compound $AB_{(s)}$ dissociates partially on melting, the true melting point is not the observed melting point. Both the observed heat of fusion and the observed melting point must be corrected to obtain the true values corresponding to the phase transition given in Eq. 9.

The corrections to the measured heat of fusion to obtain the true heat of fusion are calculated easily using the thermodynamic cycle shown in Figure 1. The first step, at point A, is to calculate the mole fraction of all species in solution at the observed melting temperature and at the bulk composition $x_1 = a_i/(a_i + b_i)$, that is, the stoichiometric composition of compound i. Secondly, z_i, the true member of moles of each component, at the observed melting point temperature, is determined from the LCPT model. Given z_i, n_i, the true number of moles of each component is calculated from $n_i = z_i n_T$, where n_T is the total true number of moles in solution. The total number of moles is calculated from an overall mass balance on the true solution: $n_T = 1/\Sigma(a_i + b_i)z_i$.

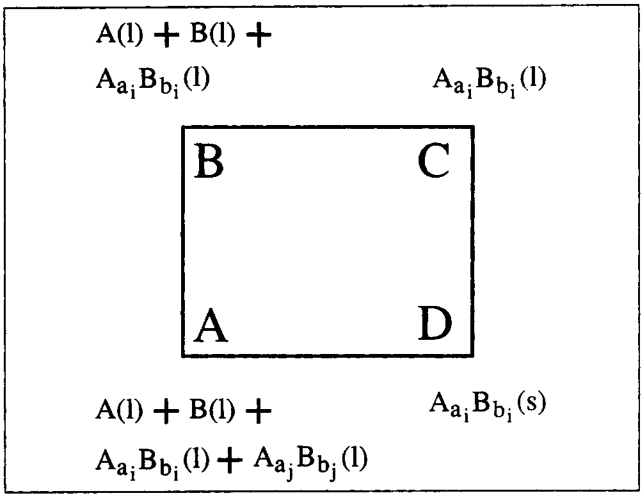

Figure 1. Thermodynamic cycle for correcting observed heat of fusion.

The objective of the thermodynamic cycle is to determine the true heat of fusion by "creating" theoretically a pure solution of compound i. To do this, all compounds, except for the compound of interest—compound i—are dissociated into monomers (points $A \rightarrow B$), and then all monomers in the solution comprising monomers and compound i are associated to form compound i (points $B \rightarrow C$), thereby forming a pure solution of compound i. Point $C \rightarrow D$ represents the phase transformation of interest, Eq. 10. The lower limits on Eqs. 11, 12, and 13 explicitly denote that compound i is excluded in these solution "transformations."

The enthalpy change from point A to B, in which all compounds except for compound i are completely dissociated, is:

$$\Delta h^{A-B} = -\sum_{\substack{j=3 \\ j \neq i}}^{N} n_j \Delta h_j^f \tag{11}$$

where Δh_j^f is the enthalpy of formation of compound j in the liquid phase. The enthalpy change from point B to C, in which all the free monomers are associated to form compound i is:

$$\Delta h^{B-C} = -\sum_{\substack{j=1 \\ j \neq i}}^{N} n_j a_j \Delta h_i^f \tag{12}$$

The enthalpy change from point D to C is the true heat of fusion, $\Delta h_{i,\text{true}}^{s-l}$, which has units of kJ/(mol $A_{a_i}B_{b_i}$). The enthalpy change from point D to A is the experimentally observed heat of fusion, $\Delta h_{i,\text{obs}}^{s-l}$, which has units of kJ/g·atom. Summing the enthalpy changes for each of the four steps in the thermodynamic cycle, the true heat of fusion is:

$$\Delta h_{i,\text{true}}^{s-l} = (a_i + b_i)\left[\Delta h_{i,\text{obs}}^{s-l} + \sum_{\substack{j=3 \\ j \neq i}}^{N} n_j \left(a_j \frac{\Delta h_i^f}{a_i} - \Delta h_j^f\right)\right] \tag{13}$$

The enthalpy change from point D to C should be evaluated

Table 3. LCPT Model Phase Diagram Representation Results

		Observed		True	
System	Compound	T^{mp} K	Δh^{fus} kJ/mol	T^{mp} K	Δh^{fus} kJ/mol
In-Sb	InSb	798	23.97	959	47.99
Cd-Sb	CdSb	729	16.11	917	32.22
Mg-Pb	Mg_2Pb	822	13.39	893	40.21
Mg-Sn	Mg_2Sn	1,043	18.62	1,177	55.86
Mg-Ge	Mg_2Ge	1,391	23.14	1,615	69.45
Au-Sn	AuSn	692	14.10	945	38.37
	$AuSn_2$	607	10.75	789	47.40
	$AuSn_4$	550	9.41	592	50.17
Ga-Mg	GaMg	646	7.78	959	33.43
	Ga_2Mg	560	7.87	617	49.04
	$GaMg_2$	723	8.12	971	42.47
	Ga_2Mg_5	743	6.86	833	62.42

at the true melting point temperature; however, since we have assumed that $\Delta C_{p,i}^{s\to l}$ is small, it is a good approximation to evaluate this difference at the observed melting point.

If the observed heat of fusion is not available, the entropy of fusion can be estimated using the procedure outlined by Kubaschewski and Alcock (1979), and the heat of fusion can be calculated knowing the observed melting point temperature.

Once a value for the true heat of fusion has been calculated, the true melting point of compound i is calculated from Eq. 14:

$$\frac{1}{T^{mp}_{i,\text{true}}} = \frac{1}{T^{mp}_{i,\text{obs}}} - \frac{R}{\Delta h^{s\to l}_{i,\text{true}}} \ln z_i\alpha_i \qquad (14)$$

In the limit where compound i does not dissociate on melting, Eq. 14 reduces to $T^{mp}_{i,\text{true}} \to T^{mp}_{i,\text{obs}}$; however, for the case when i almost completely dissociates on melting, the true melting point can be several hundred degrees greater than the observed melting point.

The crucial contribution of the LCPT model is linearization of the free energy such that there is an explicit relationship between the Gibbs energy of formation (and enthalpy of formation) and the number of atoms that comprise a compound. The physical interactions are a function of the apparent solution composition only. This relationship permits the inclusion of compounds necessary for accurate determination of the liquidus curve which were not necessary in determining the liquidus-phase properties, with no new parameters.

Phase Diagram Representation

The liquidus curve for a system is calculated from Eq. 8 after corrections to the observed heat of fusion and melting point for each compound have been made. All $z_i(T)$ and $\alpha_i(T)$ are calculated from the LCPT model equations at the liquidus temperature. Because the equations are coupled through T and $z_i\alpha_i$, an iterative calculation is required. The procedure used to calculate the liquidus temperature at a given atom fraction is initiated by calculating z_i and α_i at an assumed melting point temperature for each species in the true solution using the LCPT model. With this, the melting point temperature for each species is then calculated using the true melting point and heat of fusion. If the assumed and calculated temperatures are the same, then the iteration is complete. If the temperatures are not the same, then another iteration is done using a modified assumed temperature. Convergence is usually rapid. Finally, the liquidus curve is constructed by calculating the temperature-composition curves for all compounds and monomers using Eq. 8 and at a given atom fraction selecting the maximum temperature of those calculated.

Table 3 lists the results for the seven binary systems studied and Table 4 lists the sources for the SLE properties. The calculated liquidus curves for the seven binary systems are shown in Figures 2-8. Only compounds that are evident in the liquidus curve were considered in the SLE calculation. For example, two compounds were used to model the liquid-phase thermodynamic properties in the Mg-Pb system (MgPb and Mg_2Pb), but as seen in Figure 4 only the effect of Mg_2Pb is evident; therefore, this was the only solid-phase compound used in the evaluation of the phase diagram.

The LCPT model allows for the inclusion of additional

Table 4. Sources for Solid-Liquid Equilibria Properties

System	Compound	Δh^{fus} and T^{mp}	Phase Diagram
In-Sb	InSb	Hultgren et al. (1973)	Liu and Peretti (1952)
Cd-Sb	CdSb	Kubaschewski and Alcock (1979)	Fisher and Phillips (1954)
Mg-Pb	Mg_2Pb	Beardmore et al. (1966)	Raynor (1940); Horsley and Maskey (1957); Eldridge et al. (1965)
Mg-Sn	Mg_2Sn	Beardmore et al. (1966)	Steiner et al. (1964)
Mg-Ge	Mg_2Ge	Estimated*	Geffken and Miller (1968)
Au-Sn	AuSn	Misra et al. (1965)	Massalski (1986)
	$AuSn_2$	Estimated**	
	$AuSn_4$	Estimated**	
Ga-Mg	GaMg	Hultgren et al. (1973)	Massalski (1986)
	Ga_2Mg	Hultgren et al. (1973)	
	$GaMg_2$	Hultgren et al. (1973)	
	Ga_2Mg_5	Hultgren et al. (1973)	

*The observed melting point temperature for Mg_2Ge was obtained from Massalski (1986). The entropy of fusion was estimated using the procedure outlined in Kubaschewski and Alcock (1979) and the heat of fusion calculated using the observed melting point temperature.

**The hypothetical melting point temperatures for $AuSn_2$ and $AuSn_4$ were estimated by adding 25°C to the incongruent melting point temperatures obtained from Massalski (1986). The entropies of fusion were estimated using the procedure outlined in Kubaschewski and Alcock (1979) and the heats of fusion calculated using the hypothetical melting point temperatures.

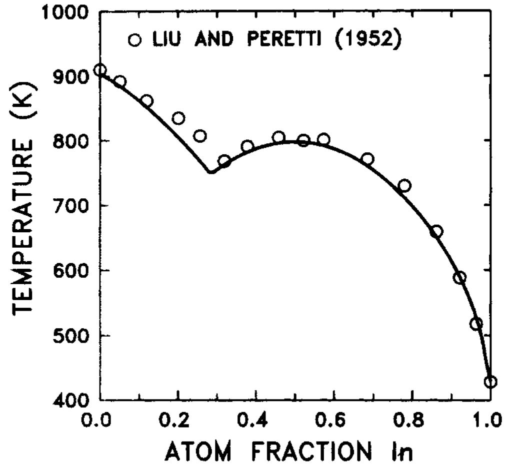

Figure 2. Phase diagram for the indium-antimony system.

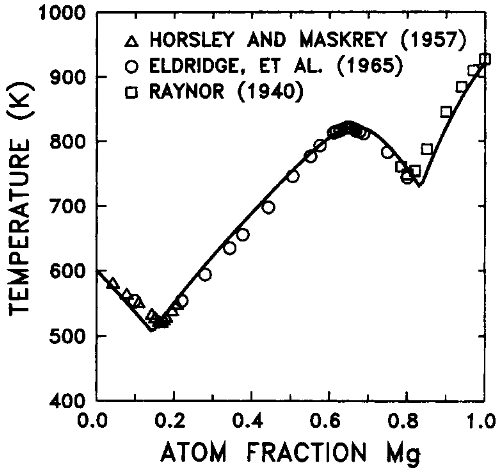

Figure 4. Phase diagram for the magnesium-lead system.

compounds in the determination of the liquidus curves that are not required for the determination of the liquid-phase properties. Two systems that demonstrate this behavior are the Au-Sn (Figure 7) and Ga-Mg (Figure 8) systems. The phase diagram of the Au-Sn system has a single congruently melting compound (AuSn) and two incongruently melting compounds ($AuSn_2$ and $AuSn_4$), which substantially affect the liquidus curve. As shown in Table 4, the observed heat of fusion and melting point temperature for the AuSn were obtained from Misra et al. (1965). The hypothetical heat of fusion and melting point temperatures for the compounds $AuSn_2$ and $AuSn_4$ were estimated by approximating the melting point temperature first for the compounds by adding 25°C to the incongruent dissociation temperature. Using the procedure outlined in Kubaschewski and Alcock (1979), the entropy of fusion for these compounds was estimated and the apparent heats of fusion were estimated using the hypothetical melting point temperature. Figure 7 shows that the agreement between the experimentally measured liquidus curve and the calculated one is surprisingly good despite the approximations required.

The SLE phase diagram for the Ga-Mg system is very interesting and relatively easy to model. All of the compounds that affect the liquidus curve melt congruently, and the heats of fusion for these compounds have been determined experimentally; therefore, neither the melting point temperatures nor the heats of fusion had to be estimated. The discrepancy between the experimentally measured liquidus curve and the calculated one could come from three sources:

(1) Errors in modeling the liquid-phase thermodynamics

(2) Errors in digitizing the phase diagram [no tabular data were available for this phase diagram; therefore, the data shown in Figure 8 were from a digitization of the phase diagram in Massalski (1986)]

(3) Experimental uncertainties.

The predominant source of error in the determination of the liquidus curves for the systems considered here is the wide range of temperatures over which the liquid-phase thermodynamic functions are calculated. To calculate the phase diagram, large-temperature extrapolations, usually down to the lowest eutectic, were required, resulting in the LCPT model predictions representing a large correction. Small changes in

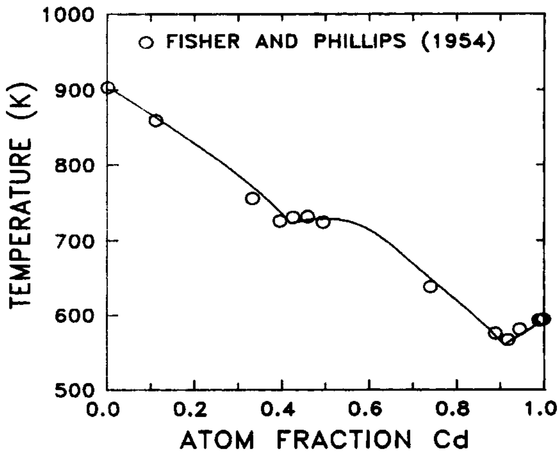

Figure 3. Phase diagram for the cadmium-antimony system.

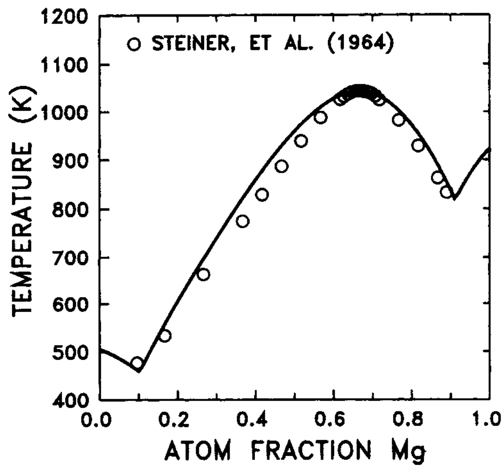

Figure 5. Phase diagram for the magnesium-tin system.

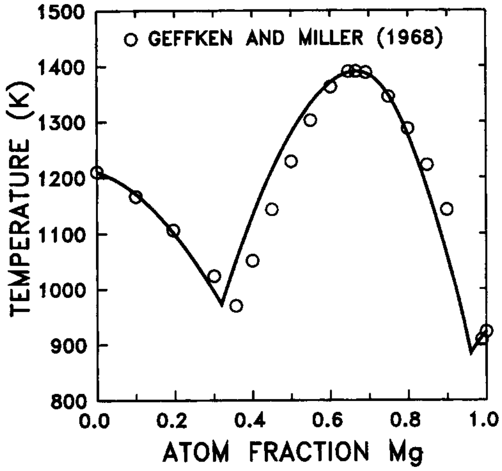

Figure 6. Phase diagram for the magnesium-germanium system.

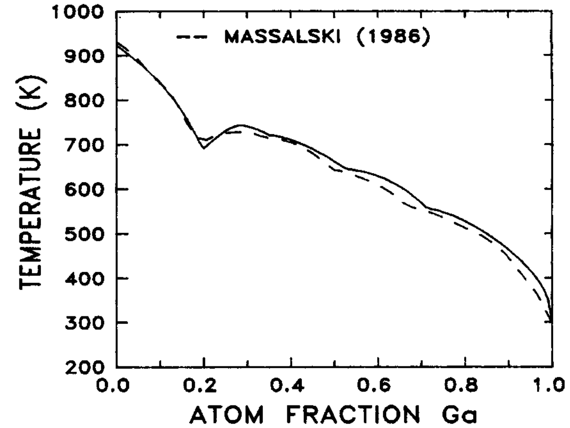

Figure 8. Phase diagram for the gallium-magnesium system.

the LCPT model parameters can affect greatly the calculated curves where such large temperature extrapolations are required. Also, we have assumed the heat of formation for the compounds, and the heat of fusion are independent of temperature. This assumption will also account for some of the discrepancy. In light of the simplifying assumptions we have used and the results obtained, we feel that the agreement is quite good.

Discussion

In this article, we have used the LCPT model to determine the liquidus curves for several compound-forming alloy systems. The basic assumptions in this treatment are that the solid phases in equilibrium with the liquid phase are pure, and the heat of fusion and liquid phase heat of formation for a compound are independent of temperature. These assumptions can be relaxed to treat more general cases at the cost of increasing the complexity of the resulting equations.

Expressions have been developed for correcting the measured heat of fusion and melting point temperature for the effects of compound dissociation on melting. We have found that the true melting point can be several hundred degrees greater than the observed melting point, while the effect of the heat of fusion is less pronounced.

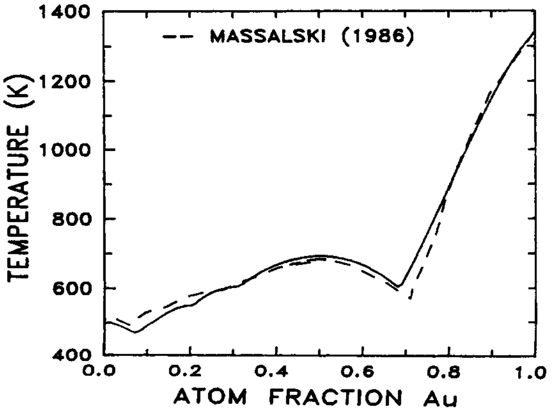

Figure 7. Phase diagram for the gold-tin system.

An analysis of the entropies of fusion, determined by dividing the enthalpy of fusion by the melting point, for the compounds in this model indicates that the entropies are generally higher than for most monatomic metals, 10–30 J/K vs. approximately 10–14 J/K. This is an indication that there are larger structural changes upon compound melting than for monatomic solids. In addition, these structural changes produce a more random structure. As denoted in Figure 1 ($D \rightarrow A$), this is the case in that not only does compound i melt (as does a monatomic solid), but additionally it dissociates, and a portion of the monomers reassociates into other compounds. The latter two structural changes are not present in the phase transformation of a monatomic solid. An analysis of the true solution composition as a function of the bulk atomic composition for a specific alloy shows (Howell and Eckert, 1987): (1) the solutions are primarily composed of monomers; (2) the amount of each compound present peaks at its stoichiometric composition; and (3) the total amount of any one compound in solution, even at its stoichiometric composition, is inversely proportional to the size of the compound. This indicates that upon melting the liquid solution is more random, in that it comprises smaller species.

The LCPT model offers a simple, easy route to determining a number of thermodynamic properties with a minimum of physically realistic parameters. The model is built on a description of the important interactions present in many liquid metal solutions. The more commonly used methods for modeling the thermodynamic properties are usually based only on simple, empirical excess Gibbs energy expressions [such as the Guggenheim strictly regular solution theory (Guggenheim, 1952)], which often require many model parameters (rarely justified by the precision of liquid metal data) to represent accurately the thermodynamic properties (Mackowiak, 1965; Gaskell, 1973). Therefore, extrapolation with the more common models is more tenuous compared with the more physically based LCPT model. In addition, since both chemical and physical interactions are included in the model, we are able to represent a wide range of liquid metal systems with a minimum of model parameters, resulting in the determination of the liquidus curves for each of these systems.

Thus, the primary advantages of the LCPT model for the description of SLE, compared with other techniques (for example, Kaufman and Bernstein, 1970), are the few number of physically realistic parameters required, ease of implementation, and wide applicability. When representing the liquidus curve, the LCPT model formulation is quite simple and provides an accurate description for systems ranging from those with single, congruent melting compounds to systems with multiple, congruently and incongruently melting compounds.

The LCPT model is useful especially for systems in which multiple compounds affect the liquidus curve, yet have a negligible effect on the liquid-phase properties. The model allows for the easy incorporation of compounds in representing the liquidus that are not necessary for representing the liquid-phase thermodynamic properties quantitatively.

The model could easily be extended to the determination of the multicomponent SLE. Howell and Eckert (1990) have presented the equations necessary for representing the liquid-phase thermodynamic properties of multicomponent alloys. It is an easy task to extend these equations, using the techniques presented here, to the representation of SLE.

Lastly, the LCPT model could be very easily modified to represent the excess functions of solid-phase species, allowing the representation of phase diagrams in which there is extensive solid-phase intermetallic compound formation.

Acknowledgment

The authors gratefully acknowledge support from the Eastman Kodak Company and Standard Oil Company (Indiana).

Notation

a, b = stoichiometric coefficients
A = interaction parameter, Scatchard equation, J/cm^3
f = fugacity, bar
f_i^o = reference state fugacity, bar
g = Gibbs energy, J
G_g = chemical interaction model parameter, J
ΔC_P^{s-l} = heat capacity difference between solid and liquid, J/K
Δh^{s-l} = enthalpy of fusion, J
Δh^f = enthalpy of formation, J
Δh^{A-B} = enthalpy change from point A to point B, J
K = equilibrium constant
n = true number of moles
R = gas constant, J/K·mol
T = temperature, K
T^{mp} = melting temperature, K
v = molar volume, cm^3
x = bulk (apparent) mole fraction
z = true mole fraction

Greek letters

α = liquid-phase true activity coefficient
γ = liquid-phase apparent activity coefficient
Φ = volume fraction

Subscripts

chem = chemical interactions
(l) = liquid
obs = observed
phys = physical interactions
(s) = solid
true = true

Superscripts

E = excess
f = fusion
mp = melting point

Literature Cited

Alger, M. M., and C. A. Eckert, "Thermodynamics of Highly Solvated Liquid Metal Solutions," *Ind. Eng. Chem. Fundam.*, **22**, 249 (1983).

Alger, M. M., and C. A. Eckert, "Simplified Chemical-Physical Theory for Liquid Metal Solutions: I. Temperature Dependence of the Gibbs Energy," *Chem. Eng. Sci.*, **41**, 2829 (1986a).

Alger, M. M., and C. A. Eckert, "Simplified Chemical-Physical Theory for Liquid Metal Solutions: II. Composition Dependence of the Gibbs Energy," *Chem. Eng. Sci.*, **41**, 2839 (1986a).

Beardmore, P., B. W. Howlett, B. D. Lichter, and M. B. Bever, "Thermodynamic Properties of Compounds of Magnesium and Group IVB Elements," *Trans. Met. Soc. AIME*, **236**, 102 (1966).

Bhatia, A. B., and W. H. Hargrove, "Concentration Fluctuations and Thermodynamic Properties of Some Compound Forming Binary Molten Systems," *Phys. Rev. B: Solid State*, **10**, 3186 (1974).

Bhatia, A. B., W. H. Hargrove, and D. E. Thornton, "Concentrations Fluctuations and Partial Structure Factors of Compound-Forming Binary Molten Alloys," *Phys. Rev. B: Solid State*, **9**; 435 (1974).

Eckert, C. A., J. S. Smith, R. B. Irwin, and K. R. Cox, "A Chemical Theory for the Thermodynamics of Highly-Solvated Metal Mixtures," *AIChE J.*, **28**, 325 (1983).

Eckert, C. A., R. B. Irwin, and J. S. Smith, "Thermodynamic Activity of Magnesium in Several Highly-Solvating Alloys," *Met. Trans. B.*, **14B**, 451 (1983).

Eldridge, J. M., E. Miller, and K. L. Komarek, "Magnesium-Lead Phase Diagram and the Activity of Magnesium of Liquid Magnesium-Lead Alloys," *Trans. Met. Soc. AIME*, **233**, 1303 (1965).

Eldridge, J. M., E. Miller, and K. L. Komarek, "Thermodynamic Properties of Liquid Magnesium-Germanium Alloys," *Trans. Met. Soc. AIME*, **236**, 1094 (1966).

Fisher, H. J., and A. Phillips, "Viscosity and Density of Liquid Lead-Tin and Antimony-Cadmium Alloys," *J. of Metals, Trans. AIME*, 1060 (Sept., 1954).

Gaskell, D. R., *Introduction to Metallurgical Thermodynamics*, McGraw-Hill, New York (1973).

Geffken, R. K., K. L. Komarek, and E. Miller, "Thermodynamic Properties and Second-Order Phase Transition of Cd-Sb Alloys," *Trans. Met. Soc. AIME*, **239**, 1151 (1967).

Geffken, R., and E. Miller, "Phase Diagrams and Thermodynamic Properties of the Mg-Si and Mg-Ge Systems," *Trans. Met. Soc. AIME*, **242**, 2323 (1968).

Gerling, U., M. J. Pool, and B. Predel, "A Contribution to the Associate Model for Binary Liquid Alloys," *Z. Metallkde.*, **74**, 616 (1983).

Guggenheim, E. A., *Mixtures*, Oxford University Press, Oxford (1952).

Horsley, G. W., and J. T. Maskrey, "1855: A Determination of the Liquidus of the System Lead-Magnesium in the Range 0-3 Weight Percent Magnesium," *J. Inst. Met.*, **86**, 446 (1957).

Howell, W. J., and C. A. Eckert, "STICT Model for Surface Thermodynamics of Liquid Metal Solutions," *AIChE J.*, **33**, 1612 (1987).

Howell, W. J., and C. A. Eckert, "Solution Thermodynamics for Liquid Metals," *Acc. Chem. Resh.*, **21**, 168 (1988).

Howell, W. J., C. T. Lira, and C. A. Eckert, "A Linear Chemical-Physical Theory Model for Liquid Metal Solution Thermodynamics," *AIChE J.*, **34**, 1477 (1988).

Howell, W. J., and C. A. Eckert, "A Linear Chemical-Physical Theory Model for Ternary Liquid Metal Solutions," *Z. Metallkde.*, **81**, 335 (1990).

Hultgren, R., P. D. Desai, D. T. Hawkins, M. Gleiser, and K. K. Kelly, *Selected Values of the Thermodynamic Properties of Binary Alloys*, Amer. Soc. for Metals, Metals Park, OH (1973).

Jordan, A. S., "A Theory of Regular Associated Solutions Applied to the Liquidus Curves of the Zn-Te and Cd-Te Systems," *Metall. Trans.*, **1**, 239 (1970).

Jordan, A. S., "Calculation of Phase Equilibria in the Ga-Bi and Ga-P-Bi Systems Based on the Theory of Regular Associated Solutions," *Metall. Trans.*, **7B**, 191 (1976).

Jordan, A. S., *Calculation of Phase Diagrams and Thermochemistry of Alloy Phases*, Y. A. Chang and J. G. Smith, eds., TMS AIME, Warrendale, PA (1979).

Kaufman, L., and H. Bernstein, *Computer Calculation of Phase Diagrams*, Academic Press, New York (1970).

Kubaschewski, O., and C. B. Alcock, *Metallurgical Thermochemistry*, Vol. 24, 5th ed., Pergamon Press, Elmsford, NY (1979).

Liu, T. S., and E. A. Peretti, "The Indium-Antimony System," *Trans. ASM*, **44**, 539 (1952).

Mackowiak, J., *Physical Chemistry for Metallurgists*, American Elsevier, New York (1965).

Massalski, T. B., *Binary Alloy Phase Diagrams*, Vols. 1 and 2, Amer. Soc. for Metals, Metals Park, OH (1986).

Misra, S., B. W. Howlett, and M. B. Bever, "On the Thermodynamic Properties of the Intermediate Phases in the System Au-Sn," *Trans. Met. Soc. AIME*, **233**, 749 (1965).

Prausnitz, J. M., R. N. Lichtenthaler, and E. G. de Azevedo, *Molecular Thermodynamics of Fluid-Phase Equilibria*, 2nd ed., Prentice-Hall, Englewood Cliffs, NJ (1986).

Predel, B., and G. Oehme, "Thermodynamic Properties of the Compound Hg_5Tl_2 and Analysis of the Enthalpies of Mixing of Liquid Mercury-Thallium Alloys with Regard to an Equilibrium of Association, *Z. Metallkde.*, **65**, 509 (1974).

Predel, B., *Calculation of Phase Diagrams and Thermochemistry of Alloy Phases*, Y. A. Chang and J. S. Smith, eds., TMS AIME, Warrendale, PA (1979).

Prigogine, I., and R. Defay, *Chemical Thermodynamics*, Longmans, Green and Co., London (1954).

Raynor, G. V., "The Constitution of the Magnesium-Rich Alloys in the Systems Magnesium-Lead, Magnesium-Tin, Magnesium-Germanium, and Magnesium-Silicon," *J. Inst. Met.*, **66**, 403 (1940).

Scatchard, G., "Equilibria in Non-Electrolyte Solutions in Relation to the Vapor Pressures and Densities of the Components," *Chem. Rev.*, **8**, 321 (1931).

Sommer, F., "Influence of Associate Formation in Alloy-Melts of Thermodynamic Quantities," *CALPHAD: Comput. Coupling Phase Diagrams Thermochem.*, **2**, 319 (1978).

Sommer, F., "Association Model for the Description of the Thermodynamic Functions of Liquid Alloys: I. Basic Concepts," *Z. Metallkde.*, **73**, 72 (1982a).

Sommer, F., "Association Model for the Description of the Thermodynamic Functions of Liquid Alloys: II. Numerical Treatment and Results," *Z. Metallkde.*, **73**, 77 (1982b).

Sommer, F., J. Lee, and B. Predel, "Temperaturabhangigkeit der Mischungsenthalpien flussiger Magnesium-Blei-und Magnesium-Zinn-Legierungen," *Z. Metallkde.*, **71**, 818 (1980).

Sommer, F., N. Rupf-Bolz, and B. Predel, "Investigation of the Temperature Dependence of the Mixing Enthalpy of Ternary Alloy Melts," *Z. Metallkde.*, **74**, 165 (1983).

Steiner, A., E. Miller, and K. L. Komarek, "Magnesium-Tin Phase Diagram and Thermodynamic Properties of Liquid Magnesium-Tin Alloys," *Trans. Met. Soc. AIME*, **230**, 1361 (1964).

Stoicos, T., and C. A. Eckert, "Nonideal Behavior in Liquid Metal Solutions: II. Physical-Chemical Theory Model," *Ind. Eng. Chem. Fundam.*, **24**, 147 (1985).

Manuscript received Oct. 7, 1991, and revision received Feb. 1, 1993.